2020 IEEE/RSJ International Conference on Intelligent Robots and Systems (IROS)
October 25-29, 2020, Las Vegas, NV, USA (Virtual)

Kinematic Optimization of an Underactuated Anthropomorphic Prosthetic Hand

Ann Marie Votta, Sezen Yağmur Günay, Brian Zylich, Erik Skorina, Raagini Rameshwar, Deniz Erdoğmuş, and Cagdas D. Onal

***Abstract*—The human hand serves as an inspiration for robotic grippers. However, the dimensions of the human hand evolved under a different set of constraints and requirements than that of robots today. This paper discusses a method of kinematically optimizing the design of an anthropomorphic robotic hand. We focus on maximizing the workspace intersection of the thumb and the other fingers as well as maximizing the size of the largest graspable object. We perform this optimization and use the resulting dimensions to construct a flexible, underactuated 3D printed prototype. We verify the results of the optimization through experimentation, demonstrating that the optimized hand is capable of grasping objects ranging from less than 1 mm to 12.8 cm in diameter with a high degree of reliability. The hand is lightweight and inexpensive, weighing 333 g and costing less than 175 USD, and strong enough to lift over 1.1 lb (500 g). We demonstrate that the optimized hand outperforms an open-source 3D printed anthropomorphic hand on multiple tasks. Finally, we demonstrate the performance of our hand by employing a classification-based user intent decision system which predicts the grasp type using real-time electromyographic (EMG) activity patterns.**

I. Introduction

The human hand is an incredibly complex mechanism that allows us to physically interact with our environment in a variety of ways [1]. Since activities of daily living can become extremely challenging for unilateral and bilateral amputees, researchers and engineers are continually working to design and improve prosthetic hands [2]. Prosthetic devices can range in complexity from a simple one degree of freedom (DoF) hook mechanism to fully articulated powered hands. Unfortunately, as complexity and functionality of a prostheses increases, so does its cost, making many of the more effective prostheses prohibitively expensive [3].

One option for decreasing costs is utilizing underactuation. With underactuation, fewer actuators are needed to drive the fingers [4], enabling researchers to create anthropomorphic, articulated hands that are relatively low in cost. Underactuation can further reduce cost by decreasing control requirements, because underactuated hands conform to objects, reducing the likelihood of damaging the object or the hand itself while grasping [5].

A significant challenge in designing prosthetic hands, underactuated or otherwise, is balancing functionality, cost, and aesthetics. In most cases, the functionality of a hand is difficult to determine until the hand has been built and tested. It would therefore be beneficial to have a methodology for objectively optimizing the hand design based on certain desired functional criteria.

While there are many instances of researchers optimizing the design of non-anthropomorphic grippers [6], [7], [8], this type of optimization is much less common among anthropomorphic hands. Kragten *et al* [9] describe a number of performance metrics that can be used to quantify an underactuated hand's ability to grasp and hold objects, with a focus on planar 2-fingered grippers. Due to the complexity of anthropomorphic hand configurations, however, it is much more difficult to determine what objective criteria should be used to gauge the effectiveness of a hand.

In [10], Feix *et al* develop a metric for comparing the motion capability of anthropomorphic hands. Their method can objectively compare similarities between robotic or prosthetic hands and the human hand, taking into account fingertip workspaces and capable hand poses. In [11], Cerruti *et al* describe an iterative numerical methodology for designing an anthropomorphic hand that achieves similar dexterity and reach to the human hand. However their solution is relatively unconstrained, and as a result would be difficult to carry out further studies beyond simulation. Authors in [12] develop an optimization metric which they call 'Interactivity of Fingers.' They create an optimized hand based on this metric, which maximizes workspace intersection between fingers and optimizes for precision grasps, but does not consider the ability to grasp larger objects.

In this paper, we present a method of kinematically optimizing the design of an anthropomorphic robotic hand. We split the optimization into two steps. First, we separately optimize the link lengths of the index, middle, ring, and pinky fingers to most closely match the 2-dimensional workspace of the corresponding human fingers. Next, using these link lengths as a starting point, we perform a 3-dimensional optimization of the entire hand to objectively determine the best positions and orientations of each finger relative to the thumb, as well as the thumb link lengths and joint angles. The hand is optimized to maximize the

A. M. Votta, E. Skorina, R. Rameshwar, and C. D. Onal are with the WPI Soft Robotics Laboratory, Mechanical Engineering Department and Robotics Engineering Program, Worcester Polytechnic Institute, MA 01609, USA. All correspondence should be addressed to Cagdas Onal cdonal@wpi.edu.

S. Y. Günay and D. Erdoğmuş are with the Cognitive Systems Lab, Department of Electrical and Computer Engineering, Northeastern University, MA 02115, USA.

B. Zylich is with the College of Information and Computer Sciences, University of Massachusetts Amherst, MA 01003, USA.

978-1-7281-6211-9/20/$31.00 ©2020 IEEE

largest object the hand can grasp while also maximizing the workspace intersection of the thumb and other fingers.

Our contributions are **(1)** a methodology to kinematically optimize an anthropomorphic hand design based on desired functional criteria, especially workspace intersection and maximum object size, **(2)** a 3D-printed anthropomorphic hand built with these optimized parameters and detailed specifications on experimentally-determined maximum object size and maximum object weight for various grasp types, and **(3)** a real-time pattern classification testing scheme to show the dexterity of the hand by accessing the user's voluntary neuromuscular drive through surface EMG signals.

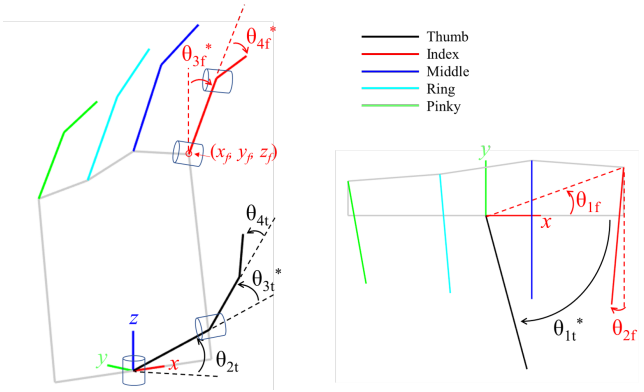

Fig. 1. Kinematic Model of the Hand.

II. Kinematic Optimization

We present our kinematic model before describing our optimization methodology. The kinematic optimization is split into two parts: **(1)** 2D optimization of the link lengths for each finger (excluding the thumb) and **(2)** 3D optimization of the finger positions and orientations and thumb geometry.

A. Kinematic Modeling

Before optimizing the hand, we first developed a kinematic model, shown in Figure 1. The hand has 5 fingers; the index, middle, ring, and pinky fingers each have 2 flexion joints, and the thumb has one joint for abduction/adduction and one for flexion. Table I shows the traditional Denavit-Hartenberg (DH) parameters for the fingers and thumb. Angles with an asterisk represent joint variables, while those without an asterisk are constant angles that are part of the finger's kinematics. The base coordinate frame is defined at the base of the thumb, meaning the thumb's base is fixed at (0, 0, 0), and the locations and orientations of the fingers are defined relative to this base frame.

B. 2D Optimization of Finger Link Lengths

For each finger (excluding the thumb), we performed a 2D optimization to maximize an objective J:

$$J = A_{H,R} - A_{H,\neg R} \tag{1}$$

TABLE I
DH Parameters

	Joint	a	α	d	θ
Fingers	1	$\sqrt{x_f^2 + y_f^2}$	0	z_f	$\text{atan2}(x_f, y_f) - \frac{\pi}{2}$
	2	0	$\frac{\pi}{2}$	0	$-\theta_1 + \frac{\pi}{2} - \theta_2$
	3	l_{f1}	0	0	θ_3*
	4	l_{f2}	0	0	θ_4*
Thumb	1	0	$\frac{\pi}{2}$	0	θ_1*
	2	l_{t1}	0	0	θ_2
	3	l_{t2}	0	0	θ_3*
	4	l_{t3}	0	0	θ_4

where $A_{H,R}$ is the overlap between the robot finger's workspace and that of the corresponding human finger and $A_{H,\neg R}$ is the area of the human finger workspace that does not overlap with the corresponding robot finger workspace. Figure 2 (a) shows the difference between a human finger workspace (3 links) and a robot finger workspace (2 links).

We parameterize each link length of each finger as some percentage w of the total length of the human finger. For example, for the robot index finger, the proximal link length (link 1) is given by $w_1(l_{pd}+l_{pm}+l_{pp})$, where l_{pd}, l_{pm}, and l_{pp} are the lengths of the human index finger's distal, medial, and proximal phalanxes, respectively. Similarly, the robot distal link length (link 2) is given by $w_2(l_{pd}+l_{pm}+l_{pp})$. Human link lengths for each finger were chosen based on the average link lengths in [13]. For each finger independently, parameters w_1 and w_2 are optimized to maximize the objective J, with the constraint that $0 \leq w_i \leq 1$. Figure 2 (b) shows how these parameters influence the objective J for one finger. However, it is not practical to do an exhaustive search for all fingers, so we use a more sophisticated optimization algorithm.

Algorithm 1: Cross Entropy Method (CEM)

Result: W_{best}, J_{best}
$W = W_0$; $\Sigma = \Sigma_0$; k; k_e; ϵ; N;
for *i=1:N* **do**
  generate_population(k, W, Σ);
  select top k_e best W's;
  $W = \frac{1}{k_e}\Sigma_{j=1}^{k_e} W_j$;
  $\Sigma = \frac{\epsilon}{\epsilon + k_e}\mathbf{I} + (W_{1:k_e} - W)^T(W_{1:k_e} - W)$;
  evaluate W; update W_{best}, J_{best};
end

For the 2D optimization, we use the Cross Entropy Method (CEM) [14] as formulated in Algorithm 1. Inputs to the algorithm are: W_0, an initial set of parameters (i.e. $W = [w_1, w_2]$), Σ_0, a covariance matrix used to randomly explore, k, the population size, k_e, the number of *elite* parameter sets to consider when updating W and Σ at each iteration, ϵ a small numerical stability constant, and N, number of iterations. We use the following inputs: W_0

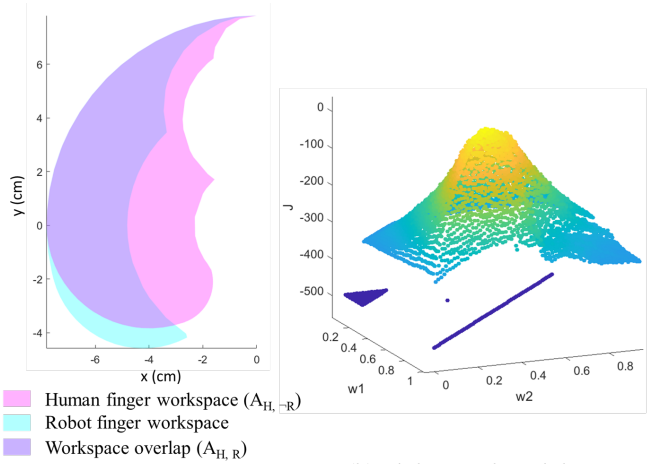

(a) Workspace Overlap

(b) Link Length Weights vs Optimization Function

Fig. 2. 2D optimization. **(a)** Overlap between human finger workspace and optimized robot finger workspace. **(b)** We plot the objective J as we vary the link length parameters, w_1 and w_2, for one finger.

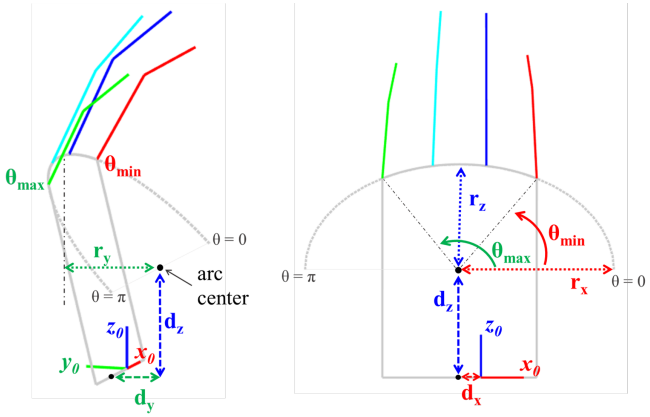

Fig. 3. 3D arc created for finger placement. Fingers are evenly spaced along arc. **Left:** Isometric view. **Right:** Front view.

uniform randomly drawn from $[0, 1]$, $\Sigma_0 = 2\mathbf{I}$, $k = 10$, $k_e = 3$, $\epsilon = 0.01$, and $N = 100$. Table III (left) shows the optimized link lengths for each finger.

C. 3D Optimization of Finger and Thumb Orientation

Using the results from the 2D optimization, we set up a 3D optimization based on the kinematic model of the hand. Because we have a large number of parameters, we used a genetic algorithm to perform the optimization.

1) Optimization Parameters: To moderately simplify the optimization, we chose to exclude the pinky finger from the analysis, as it is primarily for stability rather than grasping [15]. Later we manually chose an appropriate location and orientation. To facilitate a more anthropomorphic solution, we defined the base positions of the 3 fingers (index, middle, and ring) to be along a 3D arc (Figure 3), inspired by the distal transverse arch of the human palm [16]:

$$\begin{aligned} x(\theta) &= r_x \cos(\theta) + d_x \,|_{\theta_{min}}^{\theta_{max}} \\ y(\theta) &= r_y \sin(\theta) + d_y \,|_{\theta_{min}}^{\theta_{max}} \\ z(\theta) &= r_z \sin(\theta) + d_z \,|_{\theta_{min}}^{\theta_{max}} \end{aligned} \tag{2}$$

In total, we have 16 parameters to be optimized, defined in Table II, that describe the geometry of the robotic hand.

TABLE II
3D OPTIMIZATION PARAMETERS

Parameter	Definition
r_x, r_y, r_z	The x, y, and z radii that define the arc on which the fingers lie
d_x, d_y, d_z	The x, y, and z offsets of the arc's center from the origin
θ_{min}, θ_{max}	The minimum and maximum angles for which the arc is defined
θ_{2i}, θ_{2m}, θ_{2r}	The orientation angle of the index, middle, and ring fingers
θ_{2t}, θ_{4t}	The constant flexion angle of the thumb's metacarpal and distal phalanx
l_{1t}, l_{2t}, l_{3t}	The link lengths of the thumb's metacarpal and proximal and distal phalanxes

Because there are physical limitations on a robotic hand that must be built (e.g. links do not have zero width), and because it should not deviate too far from the size and shape of a human hand, we constrain the parameters as follows:

- The bases of the fingers must be at least 1.8 cm apart.
- The tips of the fingers must be at least 1.8 cm apart.
- The palm height (the z coordinate of each finger) must be between 9.1 cm and 12.6 cm, based on the dimensions of the human palm [17], [13], [18].
- The ring finger must have $x < 0$ to prevent the thumb from being placed below the ring or pinky fingers.

2) Optimization Objective: Our goal in optimizing our hand design is to maximize the range of object sizes the hand can grasp. We assume that if the fingertip workspace between the thumb and any finger intersects, the hand can theoretically grasp an object of zero width using the thumb and that finger. By maximizing this intersection, we increase the chances that the thumb and finger are able to meet, since each finger is underactuated and its tip position cannot be precisely controlled. For each finger, we calculate the length of the intersection curve between the 2D surfaces that define the finger and thumb workspaces. Because the index and middle fingers are more important to grasping than the ring finger [15], their intersection lengths ($l_{int,i}$ and $l_{int,m}$) are weighted by a factor of 1, while the ring finger's intersection length ($l_{int,r}$) is weighted by a lower factor of 0.75 (this weight factor is somewhat arbitrary).

To be able to also grasp large objects, we want to simultaneously maximize the object size the hand can theoretically grasp. Specifically, we calculate the maximum cylinder diameter the hand can grasp using a tripod grasp (only using index, middle, and thumb). To calculate this

maximum (cylindrical) object size, $d_{max,obj}$, we calculate the maximum object size independently for the index finger and middle finger and take the minimum of these. For the independent calculations, we consider the distance between the thumb and the finger, f, as well as the depth of the grasp, to account for object interference with the palm. For a given set of joint angles for the finger, the maximum object size that can be grasped is: $d^f_{max,obj} = \min(d^f_{max,fingers}, 2r^f_{max,palm})$, as shown in Figure 4. $d^f_{max,fingers}$ is the distance between the tip of the thumb and the tip of finger f. To calculate $d^f_{max,fingers}$ for a finger, we assign the thumb flexion angle to be zero (completely open) and determine the joint angles for the finger such that the distal link of the finger is parallel to the distal link of the thumb. $r^f_{max,palm}$ is calculated as the shortest distance from the center of the line connecting the thumb and finger tips, when their distal links are parallel, to the 'palm' plane defined by the base of the thumb and the bases of the two fingers with the greatest y-coordinates. In optimizing the object size, we only considered the hand's theoretical ability to grasp a cylinder of a given size, not weight. A more realistic calculation of maximum graspable object size would also need to consider factors such as object weight, grasp force, and friction. For our purposes, we analyzed relative finger positions as the minimum necessary condition to grasp an object but recognize that this condition alone is not sufficient to guarantee a successful grasp.

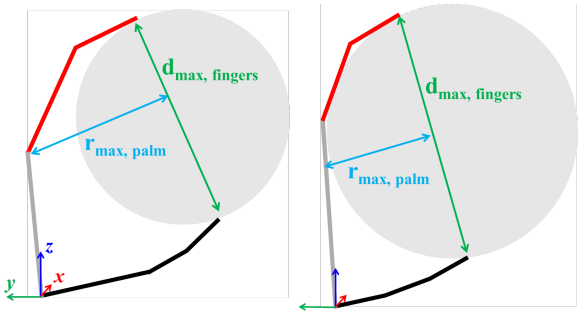

Fig. 4. Maximum Cylinder Size, side view of hand. **Left:** Maximum object size is limited by span of fingers. **Right:** Maximum object size is limited by depth of palm.

Our final optimization objective J is the product of the maximum object size and the sum of the intersection lengths between the index, middle, and ring fingers and the thumb:

$$J = \begin{bmatrix} 1 & 1 & 0.75 \end{bmatrix} \begin{bmatrix} l_{int,i} \\ l_{int,m} \\ l_{int,r} \end{bmatrix} d_{max,obj} \qquad (3)$$

3) Genetic Algorithm: For the 3D optimization, we used a genetic algorithm (GA) [19] to find the best parameters that determine finger and thumb placement and thumb link lengths. Our GA, seen in Algorithm 2, requires the following inputs; P_0: an initial population of sets of parameters ($W = [w_1, ..., w_{16}]$), k: population size, k_p: number of parents, α: exploration parameter, C: crossbreed rate, μ: mutation rate, and N: number of iterations. We use these values: P_0 includes one hand-picked parameter set and $k-1$ randomly generated parameter sets (such that all parameter sets meet constraints), $k = 30$, $k_p = 9$, $\alpha = 0.2$, $C = 0.2$, $\mu = 0.3$, and $N = 100$.

Algorithm 2: Genetic Algorithm (GA)

Result: W_{best}, J_{best}
$P = P_0$; k; k_p; α; C; μ; N;
evaluate and sort P;
for *i=1:N* **do**
  select top k_p as parents;
  for *j=1:k* **do**
    child;
    while *constraints not met* **do**
      randomly select two distinct parents;
      child = parent 1;
      with rate C over child, cross w/ parent 2;
      with rate μ over child, add $\alpha\epsilon$,
       $\epsilon \sim \mathbf{N}(0, 1)$;
    end
    P_j = child;
  end
  evaluate and sort P; update W_{best}, J_{best};
end

4) Optimized Solution: Figure 5 shows the final result of the 3D optimization, including finger workspaces (shaded) and workspace intersections (highlighted). Optimal parameter values are shown in Table III (right).

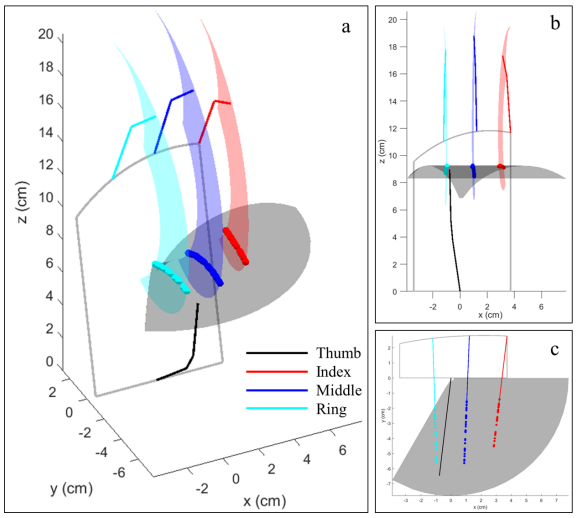

Fig. 5. Resulting hand design from the 3D Optimization. **(a)** Isometric view. **(b)** Front view. **(c)** Top view.

III. Hand Prototype Design

Our hand prototype consists of 4 fingers and a thumb, all 3D printed from PLA. Each finger link is composed

TABLE III
OPTIMIZED PARAMETERS

2D Optimization		*3D Optimization*	
Parameter	Value	Parameter	Value
l_{1i}, l_{2i}	4.8, 3.0 cm	r_x, r_y, r_z	9.6, 2.9, 12.0 cm
l_{1m}, l_{2m}	5.1, 3.8 cm	d_x, d_y, d_z	2.2, 0.0, -0.2 cm
l_{1r}, l_{2r}	4.9, 3.5 cm	θ_{min}, θ_{max}	$80.9, 125.9^\circ$
l_{1p}, l_{2p}	3.9, 2.8 cm	θ_{2i}, θ_{2m}, θ_{2r}	$6.8, 2.3, -1.8^\circ$
-	-	θ_{2t}, θ_{4t}	$38.6, 25.0^\circ$
-	-	l_{1t}, l_{2t}, l_{3t}	6.0, 1.8, 3.8 cm

of 2 PLA pieces sandwiched around a single flexible 3D printed Ninjaflex piece, which spans the length of the finger to create flexure joints. In addition to the Ninjaflex, we also embed a laser-cut PET (polyethylene terephthalate) sheet sandwiched between the PLA links to prevent lateral and torsional deformation while still allowing bending at the joints. Figure 6 shows an exploded view of the index finger. The middle, ring, and pinky fingers are identical in structure, only differing in link lengths.

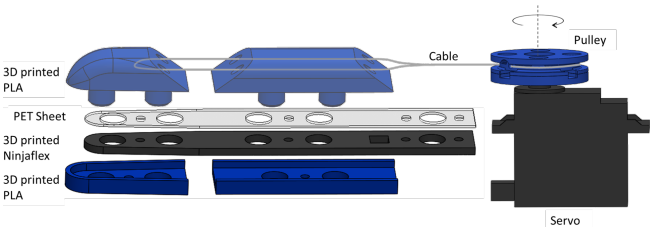

Fig. 6. Finger composed of printed PLA links and flexure joints created by printed Ninjaflex and laser-cut PLA. A cable runs through the links of the finger and is driven by a pulley attached to a Servo within the hand.

The underactuated nature of the fingers makes their behavior somewhat unpredictable, since the tip position is not actually controllable. Power grasps (multiple links of the fingers are in contact with the object) are generally more stable than precision grasps (only the fingertips contact the object). As such, we wanted to facilitate power grasps, especially with larger objects; we wanted the fingers to conform around objects, making contact with the proximal link before the second joint begins bending (Figure 7**e**). To do this, we decreased the stiffness of the flexure joint at the base of the finger compared with that of the second joint. The stiffness was decreased by removing some material from the Ninjaflex part at the location of the base joint.

In all, the hand has 5 DoF. One servo drives each of the index and middle fingers, one servo drives the ring and pinky together, and 2 servos drive the thumb for opposition and flexion motions. The fingers are tendon driven, using wire cables attached to pulleys on the servos. A similar wire-pulley setup drives the thumb's flexion motion, while its abduction/adduction is driven directly by a servo attached to its base (Figure 7**a-d**).

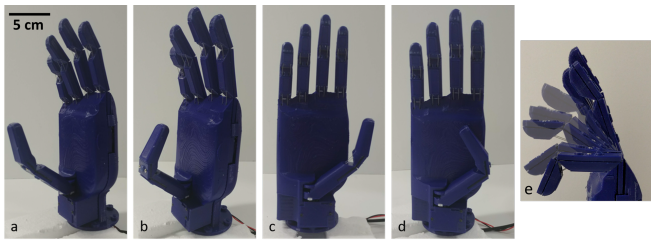

Fig. 7. **(a-d)** The thumb has 2 DoF. **(a)** Abducted and extended. **(b)** Abducted and flexed. **(c)** Adducted and extended. **(d)** Adducted and flexed. **(e)** Index finger bending. The proximal joint bends before the distal joint begins bending.

IV. EXPERIMENTS

To validate our optimization, we performed multiple qualitative and quantitative experiments to determine how well the hand can grasp objects of various sizes, how many grasp types the hand can achieve, and how quickly the hand can grasp objects when compared to the Open Bionics Ada hand [20], another open-source 3D printed design that we had available in our lab.

A. Verification of Optimization

In our optimization of the hand, the theoretical maximum and minimum object size that can be grasped are 12.6 cm and 0.0 cm respectively. After assembling the prototype hand, we experimentally determine the maximum and minimum object size to confirm the optimization results. We find that the hand is capable of grasping a cylinder with diameter 12.8 cm if assistance is provided initially to keep the object still while the hand closes around it. Without assistance, the hand is capable of grasping a cylinder with diameter 10.7 cm. This is smaller than calculated during the optimization, but this is expected because in reality, unlike in the kinematic model used for optimization, the fingers do not have zero thickness. Each finger has a thickness of 0.8 cm, except the thumb which has a thickness of 1.0 cm. The minimum object size was 0.085 cm, although the index, middle, and ring fingers can contact the thumb, so the minimum size is essentially 0 cm. As shown in Figure 8, the hand can grasp a wide variety of objects, using grasps such as pinch, lateral (key), writing tripod, and cylindrical. For the grasp types shown, we tested how much weight the hand could hold for objects of various sizes (Table IV).

B. Timed Pick and Place

We conducted an experiment to compare the time that it takes to pick and place 10 objects using the optimized hand versus the Ada hand. The 10 objects varied in shape (spherical, rectangular, cylindrical, etc.) and size (from 1.5 cm to 10.5 cm across). In this experiment, 4 participants manually positioned the hand and could open or close the hand by pressing a button. When the button (the "Enter" key on the laptop controlling the hand) was pushed, the

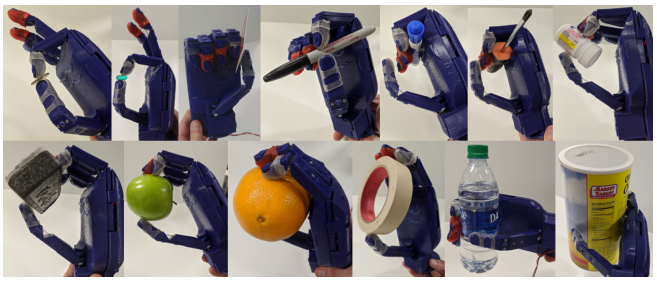

Fig. 8. The hand can grasp a wide range of everyday objects, ranging in size from 0.085 cm to 12.8 cm.

TABLE IV
MAXIMUM WEIGHT BY GRASP TYPE

Shape	Size (cm)	Grasp type	Weight (g)
Cylinder	12.8	Large diameter	430.0
Cylinder	10.7	Large diameter	455.7
Cylinder	6.67	Small diameter	413.3
Card	0.085	Lateral (key)	144.5
Box	9.63	Large diameter	209.8
Box	9.63	Medium wrap (power)	505.5
Box	4.29	Small diameter	356.6
Box	1.76	Pinch	126.5
Marker	1.07	Writing tripod	105.0

thumb would close to a pre-set position first, then all 4 fingers would close at the same time after a 0.5 s delay. Each participant had the opportunity to practice picking up 3 objects (separate from 10 test objects) until they indicated they felt comfortable, mitigating the effect of experience. Then, the participant was timed while they picked and placed all 10 objects. These steps were repeated for each prosthetic hand. Half of the participants started with the optimized hand, while half started with the Ada hand.

We found that for all 7 trials, the time it took to complete the task with the optimized hand was faster than with the Ada hand (Optimized: $\bar{x} = 59.7s$, $\sigma = 6.1s$, Ada: $\bar{x} = 97.7s$, $\sigma = 32.0s$). We noticed that the speed of opening and closing the optimized hand was faster than opening and closing the Ada hand. Thus, we calculated the time it took for each hand to open and close once (Optimized: $1.16s$, Ada: $2.86s$) and subtracted the difference (multiplied by 10 objects) from each participant's task time with the Ada hand to correct for this possible explanation of the results. Even with this correction, 5 of the 7 trials were still faster with the optimized hand (Ada corrected: $\bar{x} = 80.7s$). These results suggest that the optimized hand is able to more easily grasp a wide range of objects and is more intuitive to use.

C. Grasp Success Rate using EMG

As the final experiment, we used EMG signals for user intention detection and employed a real-time classification system to predict the gesture from 3 possible grasp types. In order to keep the classification problem relatively simple while still being able to grasp a wide range of objects, we designed the experiment using medium wrap, large diameter and pinch grasp types [27]. The resting state is also included in the gesture set for releasing the object after grasping [28].

For this experiment, the user first performed each gesture stationary for 1 second while the muscle activity was recorded using a Myo armband at 50 Hz sampling frequency. This protocol was repeated 10 times as calibration. After calibration data collection was completed, the root-mean square, mean absolute value and variance values of trials were evaluated [29] for prediction. An Extra Tree Classifier was trained using 5-fold cross-validation and learned model parameters were saved for the real-time testing experiment.

During testing, the same features were extracted for the EMG data sampled at the same frequency, and the probability distribution for the selected grasp set was calculated using the calibration model. When the calculated probability for one gesture reached 70% confidence, the grasp command was sent to the hand. To perform a pick and place task, one author selected the grasp type using the Myo armband while another author positioned the hand. We selected 3 everyday objects for each grasp type (total of 9 objects) and repeated the experiment using both the optimized hand and the Ada hand after randomizing the object order. We recorded the total time for each trial in addition to EMG misclassifications, failed grasps, and drops. The optimized hand had a grasp success rate of 93.5% (2 failed grasps and 0 dropped objects over 31 total grasp attempts), and on average it took 91.7 s to pick and place all objects. By comparison, the Ada hand had a grasp success rate of 87.5% (1 failed grasp and 3 drops over 32 total grasp attempts), with an average time of 96.7 s. The time difference between the optimized and the Ada hand is smaller in this experiment than the previous experiment, we believe, because the time taken to grasp an object is largely driven by the EMG grasp selection process. The overall EMG success rate over both experiments was 95.2%, with only 3 misclassifications over 63 grasps. The results of this experiment are similar to our prior pick-and-place experiment; the optimized hand had a higher grasp success rate and took less time to complete the task than the Ada hand.

V. CONCLUSION AND FUTURE WORK

In this paper, we proposed a new methodology for the kinematic optimization of an anthropomorphic hand based on maximizing finger workspace intersection and graspable object size. Using results from the optimization, we built a 3D printed prototype of the hand and evaluated its performance and capabilities. Our calculations suggested that the optimized hand should be able to grasp objects ranging in size from 0 to 12.6 cm, and with our prototype we successfully grasped objects ranging in size from 0.085 to 12.8 cm. We also showed that, compared to another anthropomorphic 3D-printed hand, the optimized hand grasps objects more quickly and is more successful in grasping and holding objects. Finally, we demonstrate the ability to grasp objects using real-time EMG classification to select grasp type.

TABLE V
COMPARISON WITH POPULAR PROSTHETIC HANDS

Hand	Height	Joints	Actuators	Weight	Cost
Ottobock Bebionic [21], [22]	188 mm	10	-	616 g	$\sim$ \$10,000
Ottobock Michelangelo [23], [24]	180 mm	-	-	510 g	$\sim$ \$60,000
Open Bionics Hero Arm [25], [26]	-	8	3 or 4	280-346 g	$\sim$ \$3,000
Open Bionics Ada Hand [20]	180 mm	10	5	360 g	$\sim$ \$400
Optimized hand (this study)	203 mm[1]	10	5	333 g	$<$ \$175

A major contributor to this improvement is likely the 2-DoF opposable thumb on the optimized hand. This design choice improves grasp quality and ease of grasping. Moreover, because the hand was designed to optimize its ability to grasp small and large objects, it is able to grasp a wide variety of objects more easily and quickly than the Ada hand, whose design is not optimized for grasping. Table V compares our optimized hand with some existing prosthetic hands. Our hand is significantly cheaper and fairly lightweight, although presumably much less robust than the more expensive options. Another advantage of our design methodology is that the input parameters (such as range of finger lengths or palm dimensions) of our hand can be customized for different users, resulting in a smaller or larger hand depending on the age or size of the amputee. In the future, the hand can be made more durable for practical use as a prosthetic. Furthermore, to improve performance and usability, 3D force sensors, such as those discussed in [28], can be embedded to enable force control during grasping.

ACKNOWLEDGMENT

Our work is supported by National Science Foundation (NSF) (CNS-1544636, CPS-1544895, CPS-1544636, CPS-1544815) and National Institutes of Health (NIH) (R01DC009834). This material is based upon work supported by the National Science Foundation Graduate Research Fellowship under Grant No. 1938059.

REFERENCES

[1] L. A. Jones and S. J. Lederman, *Human hand function*. Oxford University Press, 2006.
[2] B. Dellon and Y. Matsuoka, "Prosthetics, exoskeletons, and rehabilitation [grand challenges of robotics]," *IEEE Robotics Automation Magazine*, vol. 14, no. 1, pp. 30–34, March 2007.
[3] Z. Xu, *The Functional Capacity of the Humanlike Robotic Hands*. Cham: Springer International Publishing, 2019, pp. 291–312.
[4] L. U. Odhner *et al.*, "A compliant, underactuated hand for robust manipulation," *The International Journal of Robotics Research*, vol. 33, no. 5, pp. 736–752, 2014.
[5] L. Wang, J. DelPreto, S. Bhattacharyya, J. Weisz, and P. K. Allen, "A highly-underactuated robotic hand with force and joint angle sensors," in *IEEE/RSJ International Conference on Intelligent Robots and Systems*, Sep. 2011, pp. 1380–1385.
[6] L. Wen, Y. Li, M. Cong, H. Lang, and Y. Du, "Design and optimization of a tendon-driven robotic hand," in *IEEE International Conference on Industrial Technology*. IEEE, 2017-03, pp. 767–772.
[7] R. Datta, S. Pradhan, and B. Bhattacharya, "Analysis and design optimization of a robotic gripper using multiobjective genetic algorithm," *IEEE Transactions on Systems, Man, and Cybernetics: Systems*, vol. 46, no. 1, pp. 16–26, 2016-01-01.
[8] H. Dong, E. Asadi, C. Qiu, J. Dai, and I.-M. Chen, "Geometric design optimization of an under-actuated tendon-driven robotic gripper," *Robotics and Computer Integrated Manufacturing*, vol. 50, pp. 80–89, 2018-04.
[9] G. A. Kragten and J. L. Herder, "The ability of underactuated hands to grasp and hold objects," *Mechanism and Machine Theory*, vol. 45, no. 3, pp. 408–425, 2010.
[10] T. Feix, J. Romero, C. H. Ek, H. B. Schmiedmayer, and D. Kragic, "A metric for comparing the anthropomorphic motion capability of artificial hands," *IEEE Transactions on Robotics*, vol. 29, no. 1, pp. 82–93, 2013-02.
[11] G. Cerruti, D. Chablat, D. Gouaillier, and S. Sakka, "Design method for an anthropomorphic hand able to gesture and grasp," *arXiv.org*, 2015-04-05.
[12] W. S. You, Y. H. Lee, G. Kang, H. S. Oh, J. K. Seo, and H. R. Choi, "Kinematic design optimization of anthropomorphic robot hand using a new performance index," in *2017 14th International Conference on Ubiquitous Robots and Ambient Intelligence (URAI)*. IEEE, 2017-06, pp. 20–25.
[13] A. Buryanov and V. Kotiuk, "Proportions of hand segments," *Int. J. Morphol*, pp. 755–758, 2010.
[14] R. Y. Rubinstein and D. P. Kroese, *The cross-entropy method: a unified approach to combinatorial optimization, Monte-Carlo simulation and machine learning*. Springer Science & Business Media, 2013.
[15] R. W. Young, "Evolution of the human hand: the role of throwing and clubbing," *Journal of Anatomy*, vol. 202, no. 1, pp. 165–174, 2003.
[16] A. P. Sangole and M. F. Levin, "Arches of the hand in reach to grasp," *Journal of Biomechanics*, vol. 41, no. 4, pp. 829–837, 2008.
[17] J. Chang, Y.-K. Kong, A. Freivalds, H.-S. Kang, and J. H. Cho, "Investigation of relationships between hand surface dimensions and hand bone dimensions," *Proceedings of the Human Factors and Ergonomics Society Annual Meeting*, vol. 57, no. 1, pp. 948–952, 2013-09.
[18] F. Chen Chen, S. Appendino, A. Battezzato, A. Favetto, M. Mousavi, and F. Pescarmona, "Constraint study for a hand exoskeleton: Human hand kinematics and dynamics," *Journal of Robotics*, vol. 2013, no. 2013, pp. 1–17, 2013.
[19] M. Gen and L. Lin, "Genetic algorithms," *Wiley Encyclopedia of Computer Science and Engineering*, pp. 1–15, 2007.
[20] J. Raines, "Robotics hand development kit-ada v1.1-datasheet," *United Kingdom, Open Bionics*, 2016.
[21] ottobock, "bebionic hand specification sheet," 2019.
[22] A. Saenz, "How much is the newest advanced artificial hand?" *Singularity Hub*, 2015.
[23] ottobock, "Michelangelo hand technical specification," 2019.
[24] I. Birnbaum, "The 'maserati of microprocessor prosthetics' costs $120,000," *Vice*, 2016.
[25] "Hero arm - user guide," 2019.
[26] C. Jeffrey, "Open bionics' 3d-printed 'hero arm' is now available in the us," *TechSpot*, 2019.
[27] S. Y. Günay, F. Quivira, and D. Erdoğmuş, "Muscle synergy-based grasp classification for robotic hand prosthetics," in *Proceedings of the 10th international conference on pervasive technologies related to assistive environments*, 2017, pp. 335–338.
[28] A. Votta, S. Y. Gunay, D. Erdogmus, and C. Onal, "Force-sensitive prosthetic hand with 3-axis magnetic force sensors," in *IEEE International Conference on Cyborg and Bionic Systems*. IEEE, 2019.
[29] A. Phinyomark, P. Phukpattaranont, and C. Limsakul, "Feature reduction and selection for emg signal classification," *Expert systems with applications*, vol. 39, no. 8, pp. 7420–7431, 2012.

[1]Measured from the base of the thumb to the highest fingertip.